Urban Rail Transit (2017) 3(3):129–135
DOI 10.1007/s40864-017-0063-3

http://www.urt.cn/

ORIGINAL RESEARCH PAPERS

Dynamic Property Analysis of At-Ground Structure Under Moving Maglev Train

Dangxiong Wang[1] · Xiaozhen Li[1] · Jie Geng[1] · Yanlong Ge[1]

Received: 2 August 2017 / Revised: 2 September 2017 / Accepted: 4 September 2017 / Published online: 18 September 2017

Abstract In order to study the vertical coupling vibration of low–medium-speed Maglev train and at-ground structure system, the vertical coupling vibration model of low–medium-speed Maglev train-bridge system is established firstly based on the co-simulation of SIMPACK and ANSYS. The method of co-simulation is verified through the test experiments on a 20-m simply supported beam dynamic load experiment test line. Later, the vertical coupling vibration dynamics simulation model of low–medium-speed Maglev train and at-ground structure system is built and the dynamic simulation analysis is performed. According to the analysis, the vibration frequency of the at-ground structure is relatively high and the first vertical vibration frequency is 32.9 Hz; the vertical displacement and acceleration of the frame's center of the at-ground structure are bigger than the bottom's center; the vibration of the frame is the high-frequency vibration (comparing with the bottom), and the acceleration of the frame's center is obviously greater than the bottom's between 50 and 100 Hz.

Keywords Low–medium-speed Maglev train · At-ground structure · Coupling vibration · High-frequency vibration · Co-simulation

✉ Dangxiong Wang
Dangxiong333@163.com

[1] Department of Bridge Engineering, School of Civil Engineering, Southwest Jiaotong University, Chengdu 610031, China

Editor: Eryu Zhu

1 Introduction

Nowadays, with the rapid growth of China's economic and urban population, a fast, economic land occupation, environment protection way of transport is eagerly needed. Maglev transport has been born with many advantages, including well climbing capacity, small turning radius, low noise, low pollution, and good environmental compatibility. As a representative of maglev transportation, low–medium-speed maglev transportation is particularly suitable for medium–short-distance transport in cities and has good development in the future urban transportation [1].

The low–medium-speed maglev line consists of bridges and subgrade structure. Because the Maglev train embraces the rail, in subgrade section, the maglev guideway has to be propped up by a special structure and ensure the Maglev train having enough space to embracing the rail in vertical. The structure is called at-ground structure [2]. The at-ground structure is a concrete beam which is placed on the processing subgrade in advance and supported by uniform elastic subgrade, forming the combination system of Maglev train-at-ground structure subgrade. Low–medium-speed Maglev train stabilizes near the rated suspension gap through adjusting the active control electromagnetic force and keeps running smoothly. Therefore, both the bridge and at-ground structure will produce deformation under the action of Maglev train and affect the suspension gap, then affecting the smooth running of the Maglev train. Lots of scholars are all committed to Maglev train-bridge system coupling vibration: Ref. [3] analyzed the bridge dynamic responses when the high-speed Maglev train runs on the bridge at the resonance speed; Ref. [4] considering the PI control and establishing two degrees of freedom Maglev train-simply supported beam (simplified as Euler–Bernoulli beam) vertical coupling vibration model, discussed the

resonance effect of coupling model and the influences of the suspension control parameters on the coupling vibration; Ref. [5] building 10 degrees of freedom TR06 Maglev train model and simplifying the suspension control as linear spring-damping system, discussed the Maglev train-bridge vertical coupling vibration under random irregularity excitation; Refs. [6–9] establishing Maglev train-bridge vertical coupling vibration model, studied the effect of bridge stiffness, material and structure form to the dynamic responses of Maglev train-bridge system; Refs. [10, 11] analyzed dynamic characters of suspension control system and bridge and also studied the changing rules of suspension gaps at different spans and bridge stiffness; Refs. [12] considering 12 degrees of freedom Maglev train model and PD control, discussed the impact effect of Maglev train to bridge; Refs. [13, 14] analyzed the influence of wind load on the coupling vibration of Maglev train-bridge system.

The at-ground structure is supported by the uniform elastic subgrade. Under the train load, the stress mechanism is obviously different from the bridge. Under the long time operation, some uncontrollable factors will affect the Maglev train-at-ground structure vertical coupling vibration, including the supported stiffness change of subgrade, uneven settlement and the supported void. The at-ground structure is generally used frame structure, and ordinary Euler–Bernoulli beam model cannot predict the dynamic performance accurately. So, it is necessary to research the Maglev train-at-ground structure system vertical coupling vibration and the related articles is little. On the basis of predecessors' research, this paper considered the PID active suspension control and used the delicate FEM model of bridge and at-ground structure based on co-simulation of SIMPACK and ANSYS. Firstly, the Maglev train-bridge vertical system coupling vibration model was validated based on one 20-m simply supported beam load test of a low–medium-speed maglev test line. Then, the Maglev train-at-ground structure vertical system coupling vibration model was established to be analyzed.

2 Theoretical Model

2.1 The Model of Maglev Train

In this paper, the five modules low–medium-speed Maglev train was considered. Each car is supported by five pairs of suspension frames. The vehicle and suspension frame are connected through air spring, slide, etc. Each suspension frame has four independent suspension electromagnets, which produced levitation force and act on the suspension frame and bridge to achieve the maglev car suspension steady. The vehicle has 40 suspension electromagnets totally, and the neighboring electromagnets longitudinal distance is 0.7 m. Figure 1 shows the Maglev train suspension.

Car body and suspension frame are both considered six degrees of freedom. The air spring is a treated spring-damping element. The vehicle's degree of freedom is shown in Table 1, and the total number is 86. According to d'Alembent, the movement differential equations of car body and suspension frames are established [1]. Table 2 shows the main calculation parameters of Maglev train.

2.2 Suspension Control Model

The relationship among electromagnetic force, suspension gap and current is [15]:

$$F(c,i(t)) = \frac{\mu_0 A n^2}{4}\left[\frac{i_0+\Delta i(t)}{c_0+\Delta c(t)}\right]^2 \tag{1}$$

This paper considers PID control based on displacement–speed–acceleration feedback. Because the speed signal cannot be measured directly, it should be reconstructed by displacement and acceleration signals in the state observer. The state of construction is as follows:

$$\Delta\dot{\hat{c}}(t) = \Delta\dot{\hat{z}}(t) + 2\xi_0\omega_0[\Delta c(t) - \Delta\hat{c}(t)] \tag{2}$$

$$\Delta\ddot{\hat{z}}(t) = \Delta\ddot{z}(t) + \omega_0^2[\Delta c(t) - \Delta\hat{c}(t)] \tag{3}$$

After using state reconstruction, feedback current can be expressed as the function of displacement speed, acceleration feedback signal, as follows:

$$\Delta i(t) = K_p\Delta c(t) + K_v\Delta\dot{\hat{c}}(t) + K_a\Delta\ddot{z}(t) \tag{4}$$

So, the electromagnetic levitation force of control point is shown as:

$$F(c,i(t)) = \frac{\mu_0 A n^2}{4}\left[\frac{i_0+K_p\Delta c(t)+K_v\Delta\dot{\hat{z}}(t)+K_a\Delta\ddot{z}(t)}{c_0+\Delta c(t)}\right]^2 \tag{5}$$

The levitation force is applied to the electromagnet, and the active suspension control of Maglev train can be realized.

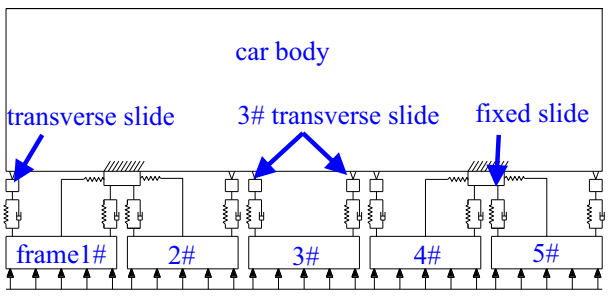

Fig. 1 Suspension of five modules *L_M*-speed Maglev train

Table 1 Dofs of the vehicle model

Component	x	y	z	α	β	γ	Remark
Suspension frame	x_{fi}	y_{fi}	z_{fi}	α_{fi}	β_{fi}	γ_{fi}	$i = 1$–10
3# sliding table	–	y_{smi}	–	–	–	–	$i = 1$–4
Other sliding tables	x_{si}	y_{si}	–	–	–	–	$i = 1$–8
Vehicle	x_{ci}	y_{ci}	z_{ci}	α_{ci}	β_{ci}	γ_{ci}	$i = 1$

Table 2 Calculation parameters of the Maglev train ($30t$)

Sign	Name	Unit	Parameters
M_c	Vehicle mass	kg	18.77×10^3
M_f	Frame mass	kg	1000
I_{cx}	Vehicle around x-axis	kg m^2	2.21×10^3
I_{cy}	Vehicle around y-axis	kg m^2	3.85×10^5
I_{cz}	Vehicle around z-axis	kg m^2	3.88×10^5
I_{fx}	Frame around x-axis	kg m^2	460
I_{fy}	Frame around y-axis	kg m^2	1150
I_{fz}	Frame around z-axis	kg m^2	1200
K_{sz}	Air spring stiffness	kN/m	80
C_{sz}	Air spring damping	kN/s/m	5

2.3 The Model of At-Ground Structure

The at-ground structure is a concrete beam which is placed on the processing subgrade in advance and supported by uniform elastic subgrade. It consists of five spans continuous rigid bridge (on top) and bottom. Subgrade consists of graded crushed stone and AB packing and the function of subgrade likes stiffness. As shown in Fig. 2, the subgrade is simplified uniform spring for theoretical model. Figure 3 shows the FE model of at-ground structure.

Because of using the modal superposition, SIMPACK eventually recognizes the modal information of at-ground structure. ANSYS has the powerful flexible body modal analysis function and can build any exquisite flexible structure model. So, for any structure (including bridge), this co-simulation method can be adopted and the theory is the same.

3 Model Validation

This co-simulation method was verified based on the 20-m simply supported beam dynamic load experiment of a test line. Using the same theory, the Maglev train-bridge vertical system coupling vibration model was established. Figure 4 shows the middle span section of the simply supported beam, using C50 concrete.

Using three Maglev train marshalings, the weight is $25t + 30t + 30t$ and the velocity of train is 80 km/h. The track irregularity spectrum recommended by Ref. [16] is adopted. Figure 5 shows the comparison of the simulation and measurement time–history curves of vertical dynamic deformation and acceleration in middle span of the simply supported beam. Figure 6 shows the comparison of the simulation and measurement frequency–history curves of acceleration in middle span of the simply supported beam.

According to the comparison, in both time–history and frequency–history, the simulation values are fit with the measured values. That is to say, the Maglev train-bridge vertical system coupling vibration model based on co-simulation method is reliable. Because of the same simulation theory, the Maglev train-at-ground structure vertical system coupling vibration model is also reliable.

4 Analysis of Maglev Train-At-Ground Structure Vertical System Coupling Vibration

4.1 Natural Frequency of At-Ground Structure

The at-ground structure FE model was established in ANSYS using solid95-type element and C40 concrete. The combin14-type element was used to simulate the uniform stiffness, and the stiffness value is 200 MPa/m. The section size is shown in Fig. 2.

Table 3 shows the nature frequency of the at-ground structure within 100 Hz. Figure 7 shows the typical vibration modes. As shown in Table 3 and Fig. 7, the nature frequencies of the at-ground structure are obviously high. There are only seven modes within 100 Hz, and the first vertical nature frequency is 32.9 Hz, and before the 32.9 Hz, there have no vertical vibration modes. The reason is the at-ground structure is supported by the strong uniform elastic subgrade and its stiffness is big. Before 80 Hz, the vibration is mainly the overall vertical modes. In the second overall vertical modes, there also has the frame's local bend vibration.

4.2 Dynamic Response Analysis of the At-Ground Structure

Using three Maglev train marshalings, the weight is $25t + 30t + 30t$ and the velocity of train is 80 km/h.

Figure 8 shows the vertical dynamic deformation in frame's center (as shown in Fig. 2, point B) and bottom's center (as shown in Fig. 2, point A) of at-ground structure. As shown in Fig. 8, the dynamic deformation time–history curves frame's center and bottom's center both have three peaks because of the three Maglev train marshalings. The maximum value is 0.466 mm (frame's center) and

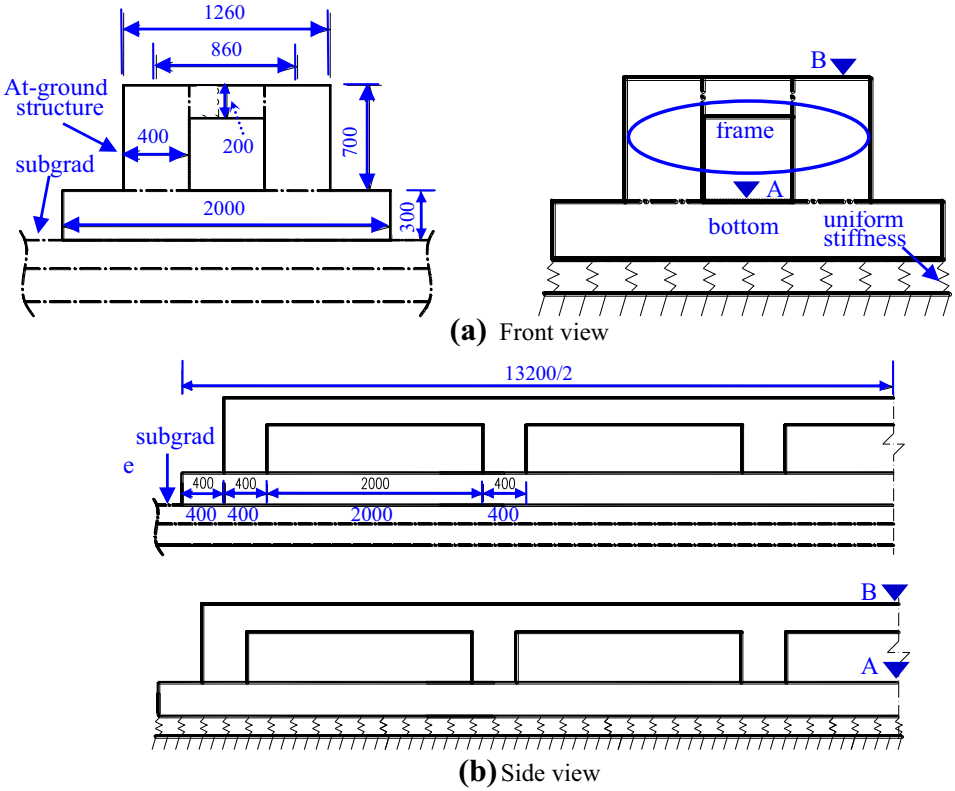

Fig. 2 At-ground structure simplified model (unit: mm). **a** Front view. **b** Side view

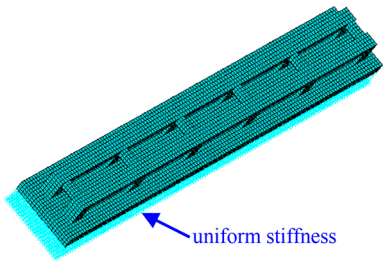

Fig. 3 At-ground structure FE model

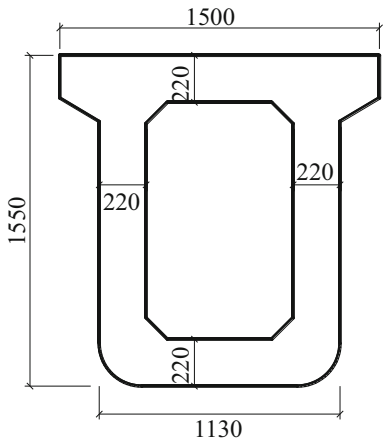

Fig. 4 Cross section of 20-m simply supported beam (unit: mm)

0.378 mm (bottom's center), respectively. Because the total dynamic deformation of frame's center is composed of the total bottom's center dynamic deformation and the local frame's center dynamic deformation, the dynamic deformation of frame's center is bigger than the bottom's center dynamic deformation.

Figure 9 shows the vertical acceleration in frame's center and bottom's center of at-ground structure. As shown in Fig. 9, the peak values of vertical acceleration in frame's center and bottom's center are 6.017 and 1.428 m/s^2. The value of frame's center is much larger than the value of bottom's center. In order to analysis the vibration characteristics of frame and bottom's center in-depth, Fig. 10 shows the acceleration frequency–history curves of frame's center and bottom's center. As shown in Fig. 10, there are obviously acceleration peaks of frame's center and bottom's center within 100 Hz and the frequency is frame's center: 31.2, 62.5, 87.8, 95.7 Hz; bottom's center: 31.2, 62.5, 95.7 Hz. Before the 50 Hz, the acceleration of frame's center is little different with bottom's center acceleration and after the 50 Hz, the acceleration of frame's center is much bigger than bottom's center acceleration.

In order to analyze the vibration, due to the natural vibration analysis of at-ground structure, the first and second frequency of vertical overall bend vibration is 32.9 and 62.4 Hz separately and at 88.2, 91.4, 97.2 Hz, there is

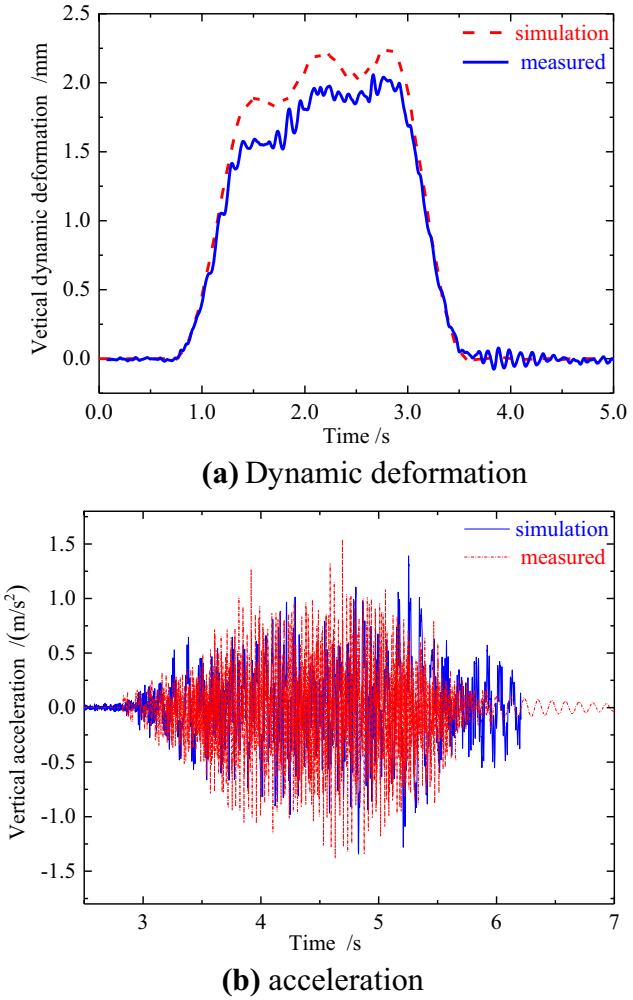

Fig. 5 Comparison of the simulation and measurement time–history curves. **a** Dynamic deformation. **b** Acceleration

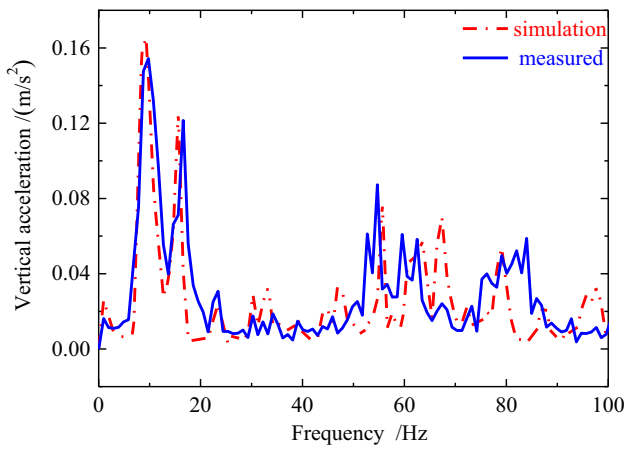

Fig. 6 Comparison of the simulation and measurement frequency–history curves

frame's local vertical vibration. So, the vibration peaks of frame's center and bottom's center are existed at this

Table 3 The modal and nature frequency of at-ground structure

Frequency	Modal
32.9	1st symmetric overall vibration
45.6	1st antisymmetric overall vibration
62.4	2nd symmetric overall vibration
77.5	2nd antisymmetric overall vibration
88.2	Frame local vibration
91.4	Frame local vibration
97.2	Frame local vibration

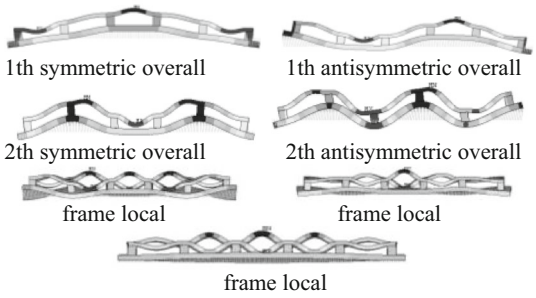

Fig. 7 The typical modal of at-ground structure

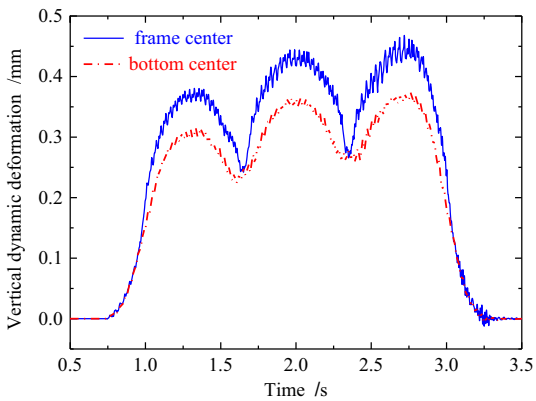

Fig. 8 The vertical dynamic displacement time–history curves of at-ground structure

frequency. From the second vertical bend modal (62.4 Hz), the frame's local vertical vibration modal appeared. So, before about 50 Hz, because of the overall vertical vibration of at-ground structure, the acceleration values of frame's center and bottom's center are nearly equal and between 50 and 100 Hz, and the acceleration of frame's center is much bigger than bottom's center acceleration based on the frame's local vertical vibration. Therefore, the frame's vertical vibration is high frequency (compared with the bottom's vibration).

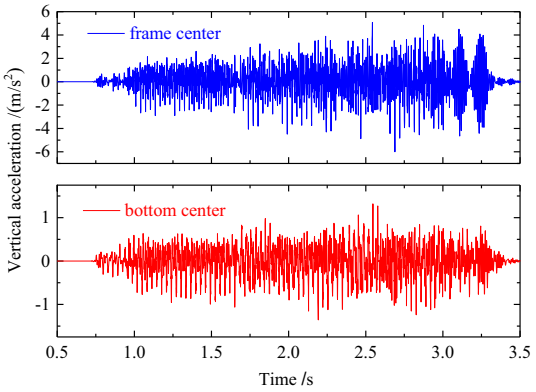

Fig. 9 The vertical acceleration time–history curves of at-ground structure

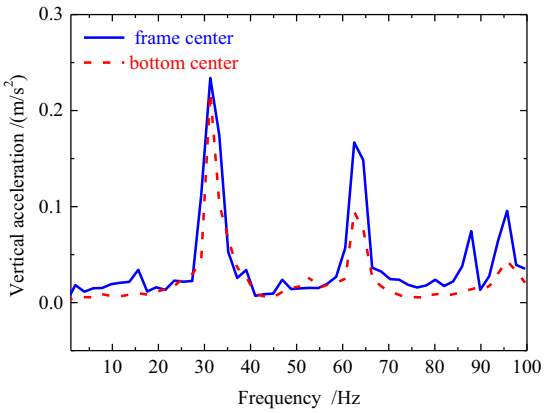

Fig. 10 The vertical acceleration frequency–history curves of at-ground structure

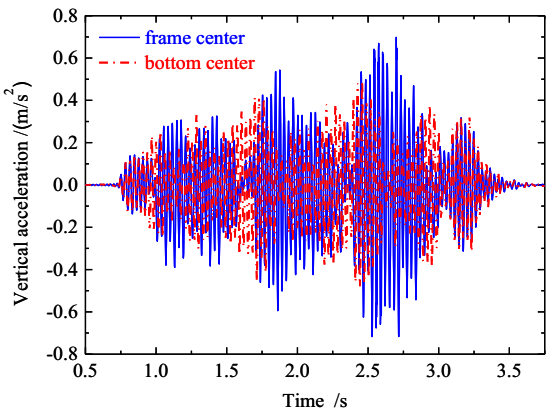

Fig. 11 The vertical acceleration of at-ground structure (50-Hz low-pass filter)

Figure 11 shows the vertical acceleration time–history curves of frame's center and bottom's center (50-Hz low-pass filter).

As shown in Fig. 11, comparing with the unfiltered curves, the 50-Hz low-pass filter acceleration curves of frame's center are little different with bottom's center acceleration curves and both the curves (50-Hz low-pass filter) have obviously three peaks (due to three Maglev train marshalings). So, although the frame's center acceleration value is much bigger than bottom's center acceleration value (unfiltered curves and time–history), it is caused by the frame local vertical vibration and the vibration is high frequency (more than 50 Hz). The different low-frequency vibration is little caused by the overall vertical vibration (less than 50 Hz). Due to the China's <High-Speed Railway Design Standard>, the bridge's limited value of vertical acceleration at ballast less track is 0.5 g considering the 20-Hz low-pass filter. The limited filter value references the European Standard. Because the vibration of frame and bottom belongs to two different frequency domains, using the filter limited value (20-Hz low-pass filter) to filter the vertical acceleration curves based on the China's <High-Speed Railway Design Standard> is slightly unsuitable.

5 Conclusions

This paper considered the PID active suspension control and used the delicate FEM model of bridge and at-ground structure based on co-simulation of SIMPACK and ANSYS. Firstly, the Maglev train-bridge vertical system coupling vibration model was validated based on one 20-m simply supported beam load test of a low–medium-speed maglev test line. Then, the Maglev train-at-ground structure vertical system coupling vibration model was established to be analyzed. The main conclusions are shown:

1. The Maglev train-at-ground structure vertical system coupling vibration model based on the co-simulation method is reliable.
2. Being supported by the strong uniform elastic subgrade, the first-order nature frequency of the at-ground structure is 32.9 Hz. Due to the frame local vibration, the acceleration of frame's center is 6.017 m/s^2, which is bigger than the bottom's center acceleration (1.428 m/s^2). The acceleration of frame's center is much bigger than the bottom's center acceleration between 50 and 100 Hz and has little difference within 50 Hz. Comparing with the vibration of bottom, the frame shows the high frequency vibration (more than 50 Hz), which lead to the acceleration of frame's center is much bigger than the bottom's center in time–history. In view of the obvious difference between at-ground structure and the conventional bridge, the vibration evaluate standard should be researched in further study.

Acknowledgements This research was supported by National Natural Science Foundation of China (NSFC, Grant Nos. 51308469, 51378429).

References

1. Deng XX (2009) The study of middle-low speed maglev vehicle system dynamic. Southwest Jiaotong University, Chengdu **(in Chinese)**
2. Wang LD (2014) Research on key technology of low and medium speed maglev guideway girder. Southwest Jiaotong University, Chengdu **(in Chinese)**
3. Shi J, Yau JD, Wang YJ (2012) Dynamic response of guideway girders due to high-speed maglev trains moving at resonant speeds. Eng Mech 29(12):196–203 **(in Chinese)**
4. Yau JD (2009) Vibration control of maglev vehicles traveling over a flexible guideway. J Sound Vib 321:184–200
5. Zhao CF, Zhai WM (2002) Maglev vehicle/guideway vertical random response and ride quality. Veh Syst Dyn 38(3):185–210
6. Cai CB (2001) Maglev vehicle/elevated-beam guideway vertical coupling dynamics. J China Railw Soc 23(5):27–33 **(in Chinese)**
7. Shi J, Wei QC, Wu FY (2003) Study on vibration of the beam of magnetic levitation express railway and its control. China Saf Sci J 10:76–80 **(in Chinese)**
8. Jiang WL, Gao MM (2004) Study of the effect of track beam parameters on vertical coupled dynamic response of maglev vehicle-viaduct. China Railw Sci 25(3):71–75 **(in Chinese)**
9. Lee JS, Kwon SD, Kim MY et al (2009) A parametric study on the dynamics of urban transit maglev vehicle running on flexible guideway bridges. J Sound Vib 328(3):301–317
10. Zhai WM, Zhao CF (2005) Dynamics of maglev vehicle/guideway systems (I)—magnet/rail interaction and system stability. Chin J Mech Eng 41(7):1–10 **(in Chinese)**
11. Zhai WM, Zhao CF (2005) Dynamics of maglev vehicle/guideway systems (II)—modeling and simulation. Chin J Mech Eng 41(8):163–175 **(in Chinese)**
12. Shan CS (2014) Study on vertical coupling vibration of low-medium speed maglev train-bridge system. Southwest Jiaotong University, Chengdu **(in Chinese)**
13. Yau JD (2009) Aerodynamic vibrations of a maglev vehicle running on flexible guideways under oncoming wind actions. J Sound Vib 329:1743–1759
14. Kwon SD, Lee JS, Moon JW et al (2008) Dynamic interaction analysis of urban transit maglev vehicle and guideway suspension bridge subjected to gusty wind. Eng Struct 30:3445–3456
15. Shi J, Wei QC, Zhao Y (2007) Analysis of dynamic response of the high-speed EMS maglev vehicle/guideway coupling system with random irregularity. Veh Syst Dyn 45(12):1077–1095
16. Liang X (2015) Study on maglev vehicle/guideway coupled vibration and experiment on test rig for a levitation stock. Southwest Jiaotong University, Chengdu **(in Chinese)**